Int. J. Electrochem. Sci., 11 **(2016)** 6477 – 6490, doi: 10.20964/2016.08.57

International Journal of ELECTROCHEMICAL SCIENCE
www.electrochemsci.org

Facile Synthesis of Bimetallic Pt_xCu_{1-x} Nanostrands and Their Application in Non-Enzymatic Glucose Sensor

Tingting Guo[1#], *Yu Zhang*[1#], *Yuejun Ouyang*[2,*], *Gang Yu*[1,*], *Yuan Liao*[1], *Ziping Zhang*[3]

[1] State Key Laboratory of Chemo/Biosensing and Chemometrics, College of Chemistry and Chemical Engineering, Hunan University, Changsha 410082, PR China
[2] Huaihua Key Laboratory of Functional Inorganic & Polymeric Materials, Huaihua University, Huaihua, 418000, PR China
[3] College of life science, Yantai University, Yantai, 264005, PR China
[*]E-mail: yuganghnu@163.com, oyyj0816@163.com
[#] Co-first-author, they contributed equally to this work

Received: 30 April 2016 / *Accepted:* 17 June 2016 / *Published:* 7 July 2016

Bimetallic Pt_xCu_{1-x} nanostrands were fabricated through a facile and effective wet chemical strategy and modified on glassy carbon electrode for sensitive non-enzymatic glucose sensors. Physical properties of the Pt_xCu_{1-x} nanostrands were characterized by transmission electron microscopy (TEM), scanning electron microscopy (SEM) combined with energy dispersive X-ray spectroscopy (EDS), and X-ray diffraction (XRD) techniques. Electrochemical performances of the Pt_xCu_{1-x} nanostrands were evaluated by cyclic voltammetry, electrochemical impedance spectroscopy and chronoamperometry and compared to Pt nanostrands when modified onto glassy carbon electrodes. Electrochemical measurements indicated that the oxidation current of glucose on the $Pt_{70}Cu_{30}$ nanostrands modified electrode is linear to its concentration from 0.1 to 19 mM with a detection limit of 25 μM (*S*/*N*=3) and a good sensitivity of 23 $\mu A \cdot mM^{-1} \cdot cm^{-2}$. Besides, the $Pt_{70}Cu30$ nanostrands modified electrode can avoide the interference of ascorbic acid (AA), uric acid (UA), acetamidophenol (AP) and fructose. And it also demonstrated superior selectivity, outstanding stability, attractive reproducibility, and well feasibility for the analysis of real sample. Benefiting from its wonderful electrochemical performance, low spend as well as ease in fabrication, this novel $Pt_{70}Cu_{30}$ nanostrands material provides a potential candidate for preparing non-enzymatic glucose sensors with good properties.

Keywords: Electrocatalysis; Pt_xCu_{1-x} nanostrands; Glucose; Non-enzymatic sensor

1. INTRODUCTION

Diabetes has become one of the leading diseases causing disability and death, and it will be the 7th main cause of death in the year of 2030. According to the World Health Organization, there are 347 million people suffering from this disease [1]. When the individual suffers from metabolic disorder caused by obesity, the concentration of glucose in his blood would be high. Glucose is the key

characteristic components in the life process, its analysis plays a quite important role on the diagnosis and management of human's healthy, especially for diabetes mellitus [2]. Thus, it is meaningful to prepare fast, stabilized and exact sensors for detecting glucose. Glucose enzyme biosensors with high sensitivity and good selectivity have been first developed [3]. However, they are easily influenced by ambient conditions, for example, humidity, temperature, pH, toxic chemicals and ionic detergents [4, 5], which leads to the disadvantages of insufficient long-term stability and unsatisfactory reproducibility [6] .

To overcome these problems, non-enzymatic glucose amperometric sensors, with direct electrocatalytic oxidation of glucose at an enzyme-free electrode have attracted considerable attention because of their simplicity, short response time and high sensitivity [7]. Numerous non-enzymatic glucose sensors have been reported [8-12]. Among them, Pt-based amperometric sensors are becoming the promising approaches [13], because the Pt-based nanomaterials with large surface areas and high electrocatalytic activities are very desirable for such non-enzymatic sensors [14]. For example, Pt-M (M=Ag, Cu, Ir, Fe) alloy nanomaterials have exhibited enhanced catalytic performances compared with commercial Pt catalysts or Pt wire [14-18] . However, the expensive cost for Pt has restricted its practical application. Therefore, the search for materials cheaper than Pt finds growing research interest and considerable attention has been focusing on Cu-based materials owing to their good electron transfer along one-dimensional(1-D) direction and great mechanical strength [19]. For instance, 1-D assembly of Cu nanoparticles and Cu nanowires have been synthesized and applied to the non-enzymatic determination of glucose, which showed better sensing property compared to their zero-dimensional counterpart [20, 21]. Because bimetals are more beneficial for enhancing catalytic properties through synergistic interactions, we infer that the combination of Pt and Cu can not only reduce the spending, but also enhance the electrocatalytic performance for glucose detection. As is well-known, there already have been several reports about enzyme-free glucose sensors based on PtCu nanocompositions [17, 22]. Despite the improved catalytic performances of PtCu nanocompositions, the previous methods for synthesis of these nanocompositions were either carried out with poisonous reagents or needed complicated procedures. In short, the goal of facile preparation of PtCu nanocompositions for sensitive non-enzymatic glucose sensors remains largely unmet.

In this paper, we prepared bimetallic Pt_xCu_{1-x} nanostrands through a facile and effective wet chemical strategy and employed them as electrode material for enzymatic-free glucose sensors. The prepared bimetallic Pt_xCu_{1-x} nanostrands modified electrodes exhibited fast response, good sensitivity, low detection limit, superior selectivity, outstanding stability and attractive feasibility for real sample analysis. Due to its ease in preparation, low expenditure and fantastic performance for glucose detection, this class of bimetallic Pt_xCu_{1-x} nanostrands modified electrode provides a very promising candidate for non-enzymatic glucose sensor.

2. MATERIAL AND METHODS

2.1. Chemicals

K_2PtCl_6, $NaBH_4$, NaOH, $Cu(NO_3)_2{\cdot}2H_2O$ and Triton X-100 were obtained from Sinopharm Chemical Reagent Co. Ltd (shanghai, China). Glucose was purchased from Kermel Chemical Reagent

Co. Ltd of Tianjin. All chemical reagents, unless otherwise stated, were of analytical grade and did not been further purified before using. Deionized water (18.2 MΩ cm) was used throughout the experiments.

2.2. Synthesis of PtCu nanostrands

The PtCu dimetallic nanostrands were synthesized by co-reduction of the potassium chloroplatinate and copper chloride hydrate with $NaBH_4$ in an aqueous solution. In a typical synthesis of $Pt_{70}Cu_{30}$ nanostrands, 1 mL of 5 mM K_2PtCl_6, 1 mL of 1 mM $Cu(NO_3)_2$ and 1mL of 1 $mg{\cdot}mL^{-1}$ Triton X-100 aqueous solutions were added to 10 mL of 10 M NaOH aqueous solution under continuous stirring, and the mixture was further stirred under argon for 1 h. Then a proper amount of $NaBH_4$ solution was quickly injected into the mixture. After stirring for 1 min, the reactor was then placed in a water bath of 60℃ for 1 h to obtain a black dispersion. The black dispersion was centrifuged, and the solid was washed several times with deionized water and ethanol, respectively. After that, the obtained powder was dispersed in ethanol for further use. Other different composites of Pt_xCu_{1-x} nanostrands ($Pt_{80}Cu_{20}$, $Pt_{50}Cu_{50}$) were synthesized with the similar method with diverse Pt/Cu atomic ratios (7:1, 5:4). And Pt nanostrands were prepared for comparison by a similar synthetic method without adding potassium chloroplatinate.

2.3. Preparation of PtCu nanostrands modified electrodes

To fabricate the modified electrodes, a glassy carbon electrode (GCE, d=5 mm) was polished sequentially with 0.3 and 0.05 μm Al_2O_3 powder and rinsed by ethanol and deionized water. Then, 5 μL of 5 $mg{\cdot}mL^{-1}$ PtCu nanostrands suspension in ethanol was dropped onto a GCE electrode surface. After drying, 10 μL of Nafion solution (0.5 wt% in ethanol) was coated on the surface of PtCu nanostrands to avoid PtCu nanostrands leakage. The as-prepared PtCu nanostrands modified electrodes were denoted as Pt_xCu_{1-x}GCE. Furthermore, Pt nanostrands modified electrodes were prepared with the same method.

2.4. Apparatus and electrochemical measurements

The morphologies of PtCu nanostrands were characterized by field emission scanning electron microscope (FE-SEM, Hitachi S-4800) operated at 10 kV. Surface elemental composition of the synthesized PtCu nanostrands was characterized by an energy dispersive X-ray spectrometer (EDS, Horiba 7021-H). The microstructures of PtCu nanostrands were performed by high-resolution transmission electron microscope (HRTEM) and selected area electron diffraction (SAED, JEM-3010). The powder X-ray diffractometer patterns were obtained using a Shimadzu X-ray diffractometer instrument (XRD, Shimadzu-6100) operating with Cu Kα (λ=0.154 nm) radiation.

All the electrochemical tests were accomplished on an electrochemical workstation (Gamry Instruments, Interface1000) in a three-electrode system equipped with a saturated calomel reference

electrode (SCE), a Pt wire auxiliary electrode and the modified electrode as a working electrode. All potentials were reported with respect to the SCE throughout this paper. The electrochemical glucose detection performance was investigated by the cyclic voltammetry (CV) measurement, electrochemical impedance spectroscopy (EIS) technique and chronoamperometry (*I*-t).

3. RESULTS AND DISCUSSION

3.1. Characterization of Pt_xCu_{1-x} nanostrands

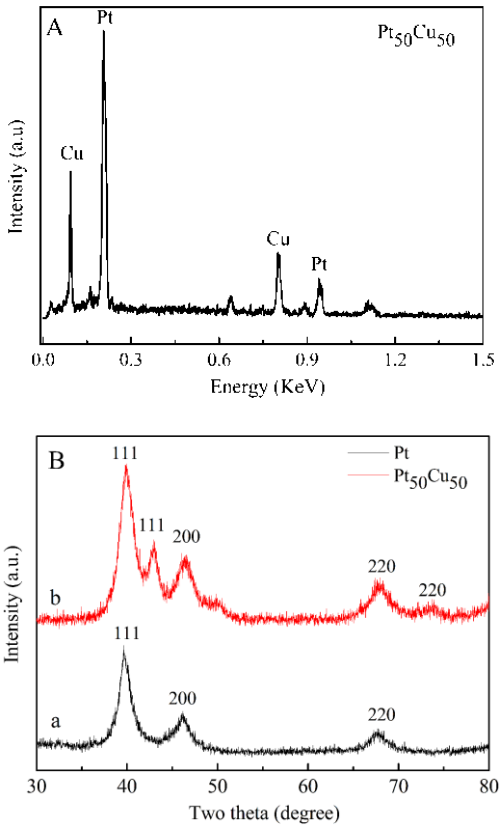

Figure 1. (A) the EDS spectrum of $Pt_{50}Cu_{50}$, (B) typical XRD patterns of (a) Pt, (b) $Pt_{50}Cu_{50}$.

Fig. 1A shows the EDS spectrum of the as-prepared PtCu nanocomposites. It exhibits that the atomic percentage of the Pt is about 50%. Fig. 1B shows the XRD patterns of the Pt and PtCu nanocomposites, respectively. For the Pt sample (black curve), the major diffraction peaks for Pt sample (black curve) at 2θ=39.8°, 46.2° and 67.5°can be well indexed as face-centered cubic (fcc) Pt (JCPDS card no. 04-0802). As shown in the red curve in Fig. 1B, the diffraction peaks of PtCu nanostrand composites match well with the combined spectra of Pt (JCPDS card no. 04-0802) and Cu (JCPDS card no. 04-0836). Note that no diffraction peaks of PtCu alloy have been observed, which indicates that as-synthesized PtCu composites are bimetal instead of alloy. [12]. The cause of this result might be related to the different nucleation rates of Pt and Cu during the reduction of K_2PtCl_6 and $Cu(NO_3)_2$ with $NaBH_4$ [23].

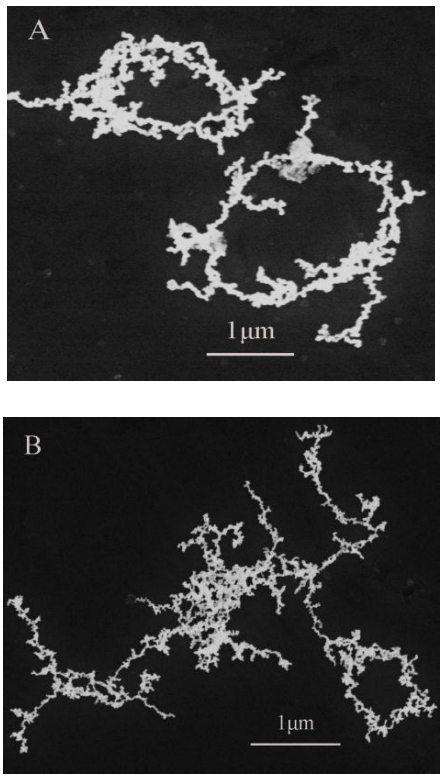

Figure 2. Typical SEM images of as-prepared (A) Pt nanostrands , (B) PtCu nanostrands.

Fig. 2 shows the morphologies of the as-prepared Pt and PtCu nanocomposites obtained by SEM. Non-uniform, flexural strand-like morphology constructed by a series of nanoparticles was observed on the as-synthesized Pt samples (Fig. 2A). In Fig. 2B, it could be clearly seen that high-quality PtCu nanostrands are formed, and no separated nanoparticle was occurred throughout the whole area of observation. The synthesized PtCu nanostrands are hundreds of nanometers in length and their average diameter is about 20 nm. In comparison with Fig. 2A, PtCu nanocomposite has a similar morphology as Pt nanostrands, whereas the size of PtCu is obviously smaller than that of Pt. In addition, the morphology of PtCu is more uniform than that of Pt nanostrands. Owing to its unique nanostructure, we speculate that the PtCu nanostrands will be beneficial for the electrochemical oxidation of glucose.

The TEM and HRTEM characterizations give a further insight into the microstructures of the as-prepared PtCu nanostrands. As shown in Fig. 3A, the synthesized PtCu nanostrands are constituted with a series of nanoparticles, which agrees well with the SEM characterization.

According to the HRTEM lattice image of PtCu sample shown in Fig. 3B, the lattice fringe distances of 0.209 nm and 0.227 nm could be identified as the (111) lattice spacing of fcc Cu (JCPDS card no. 04-0836) and fcc Pt (JCPDS card no. 04-0802), respectively. These results can be matched well with the calculated values of 0.209 nm for Cu and 0.227 nm for Pt based on XRD information. And the inset of Fig. 3B is the SAED pattern with several bright concentric rings that could be attributed to PtCu crystal diffractions.

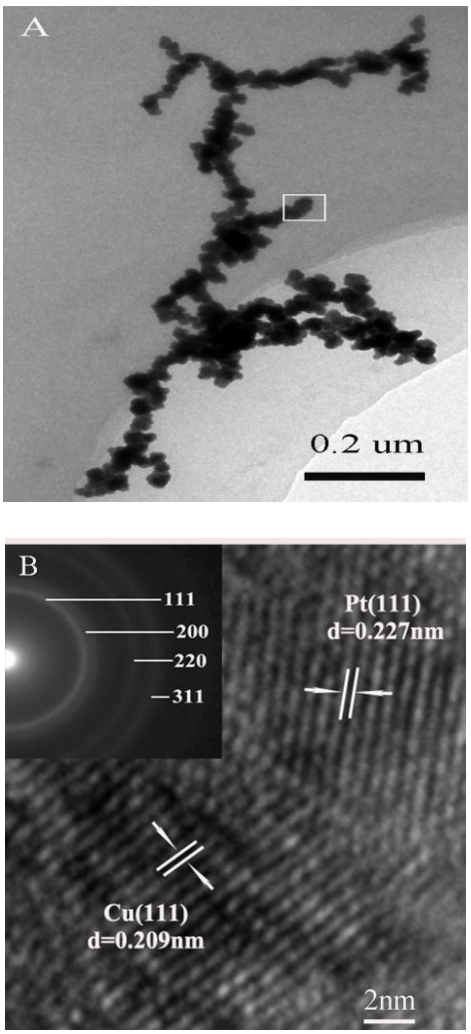

Figure 3. (A) Typical TEM images of PtCu nanostrands, (B) HRTEM images of the PtCu nanostrands and inset is the SAED patterns.

3.2. Electrochemical behaviors of the Pt_xCu_{1-x} nanostrands modified electrodes

The electrochemically active surface areas (ECSA) could be applied to evaluate the electrochemical behaviors of the Pt_xCu_{1-x} nanostrands. As shown in Fig. 4A, it demonstrates the cyclic voltammetry curves of Pt_xCu_{1-x}GCE electrodes and the PtGCE electrode, which were carried out in 0.5 M H_2SO_4 solution at a scan rate of 50 $mV \cdot s^{-1}$.

By means of measuring the charges collected in the Hupd adsorption/desorption region after double-layer correction and assuming a value of 210 $\mu C \cdot cm^{-2}$ for the adsorption of a hydrogen monolayer [24], the ECSA of the nanomaterials were calculated to be 9.87 $mC \cdot cm^{-2}$ ($Pt_{70}Cu_{30}$GCE), 8.59 $mC \cdot cm^{-2}$ ($Pt_{80}Cu_{20}$GCE), 4.56 $mC \cdot cm^{-2}$ ($Pt_{50}Cu_{50}$GCE), 3.25 $mC \cdot cm^{-2}$ (PtGCE), respectively. The results suggest that the ratio of Pt and Cu can significantly affect the electrochemical activity of PtCu nanocomposites.

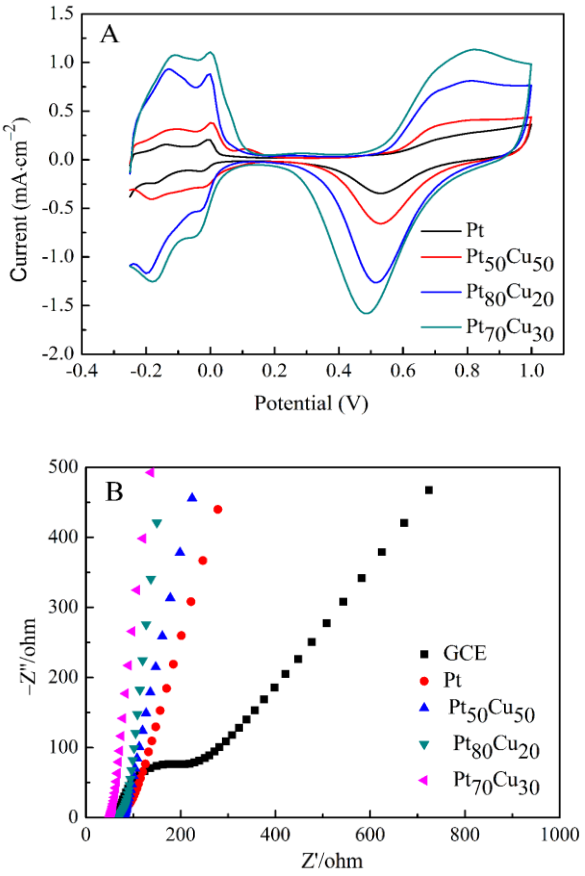

Figure 4. (A) Cyclic voltammograms of the Pt_xCu_{1-x}GCE electrodes and the PtGCE electrode in 0.5 M H_2SO_4 solution; (B) Electrochemical impedance spectroscopy of Pt_xCu_{1-x} nanostrands, Pt nanostrands, bare GCE in 5 mmol·L^{-1} $[Fe(CN)_6]^{3-}$/$[Fe(CN)_6]^{4-}$ containing 0.1 mol.L^{-1} KNO_3. AC voltage: 5 mV; frequency range: 0.01 Hz~100 kHz.

Electrochemical impedance pectroscopy (EIS) was a typical technique for verifying the electrochemical activity of the modified electrodes and studying the interface properties of electrode surfaces. Fig. 4B displays the EIS of Pt_xCu_{1-x}GCE, PtGCE and bare GCE in 5 mmol·L^{-1} $[Fe(CN)_6]^{3-}$/$[Fe(CN)_6]^{4-}$ containing 0.1 mol·L^{-1} KNO_3. As shown in Fig. 4B, a squeezed semicircle at high frequency corresponding to the electron transfer limited process could be observed for all of the electrodes. And a linear part at the low frequency was caused by the diffusion controlled process. In addition, each semicircle diameter at the high frequency represented electron transfer resistance (R_{ct}) of the corresponding electrode surface. It was shown that the electron transfer resistance of the electrodes decrease in the order of bare GCE (95 Ω) > Pt (30 Ω) > $Pt_{50}Cu_{50}$ (20 Ω) > $Pt_{80}Cu_{20}$ (15 Ω) > $Pt_{70}Cu_{30}$ (5 Ω). These results implied that the Pt_xCu_{1-x}GCE electrodes were more favourable for electron transfer compared with Pt electrode. Furthermore, the R_{ct} of $Pt_{70}Cu_{30}$ was smaller than that of $Pt_{80}Cu_{20}$, which agreed with the results deduced from ESCA.

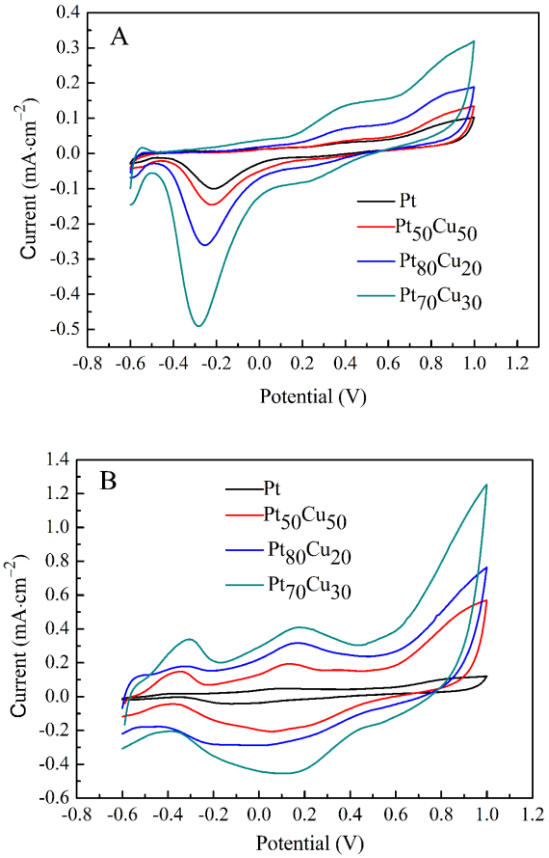

Figure 5. Cyclic voltammograms of the Pt_xCu_{1-x}GCE electrodes and the PtGCE electrode in (A) 0.1 M PBS containing 0.15 M NaCl (pH=7.4) and (B) 0.1 M PBS containing 0.15 M NaCl with 10 mM glucose (pH=7.4). Scan rate: 20 mV·s^{-1}.

The electrochemical activities of the Pt_xCu_{1-x}GCE electrodes for electrochemical oxidation of glucose were tested by cyclic voltammetry. For this test, 0.1 M phosphate-buffered saline (PBS) solution containing 0.15 M NaCl (0.1 M PBS/0.15 M NaCl, PH=7.4) was chosen as the electrolyte as it is comparable to physiological conditions. Fig. 5A presents cyclic voltammograms of the Pt_xCu_{1-x}GCE electrodes in the phosphate buffer without glucose. Except with the different current densities, the voltammograms behave similarly. The anodic peak which corresponds to metal oxide formation shows up at about 0.4 V, and the cathodic peak that relates to metal oxide reduction appears at about −0.28 V. As shown in Fig. 5B, upon addition of 10 mM glucose, the voltammetric characteristics of Pt_xCu_{1-x}GCE electrodes alter significantly and display a quite complicated electrochemical behavior. Two anodic peaks at −0.35 V and 0.15 V are found in the positive scan, which results from the oxidation of glucose. In the negative scan, owing to the presence of the surface oxide, the oxidation of glucose is suppressed.

Because of the reduction of surface Pt oxide, an increasing number of surface active sites should be used to oxidize glucose once again. These phenomena can be explained by a well-accepted mechanism of glucose oxidation on a Pt electrode in neutral media [25, 26]. According to the above results, it could be observed that the $Pt_{70}Cu_{30}$ modified electrode exhibits the best electrocatalytic activity toward the oxidation of glucose.

The catalytic characteristics of the bimetallic Pt_xCu_{1-x} toward the oxidation of glucose could be rationalized by the following mechanism. Primarily, the glucose is decomposed into gluconate or other intermediates (RO) and these species could be adsorbed on active Pt sites with slow oxidation [27]. Thus, the enhanced catalytic property of Pt_xCu_{1-x} electrode may be attributed to two causes: one is the increase in electroactive platinum species, which was caused by the addition of copper [28]. In other word, Cu could be beneficial for desorption of the oxygenated species (OR), which finally generate the Cu-OR species. The other is that the incorporation of Cu can weaken the strength of the Pt-RO bond, and this greatly facilitates the regeneration of Pt sites [29, 30].

3.3. Amperometric response of the $Pt_{70}Cu_{30}$GCE electrode to glucose

The $Pt_{70}Cu_{30}$GCE electrode was then used for electrochemical detection of glucose. It is well-known that the detection potential can significantly influence the amperometric responses of amperometric sensors. In order to obtain the optimized potential, we have investigated the effect of detection potential on the current responses of $Pt_{70}Cu_{30}$GCE electrode to various concentrations of glucose. Two oxidation potentials of –0.35 V and 0.15 V were tested. As shown in Fig. 6A, in both curves, the current semaphores increased promptly after the glucose was added into the stirred solution.

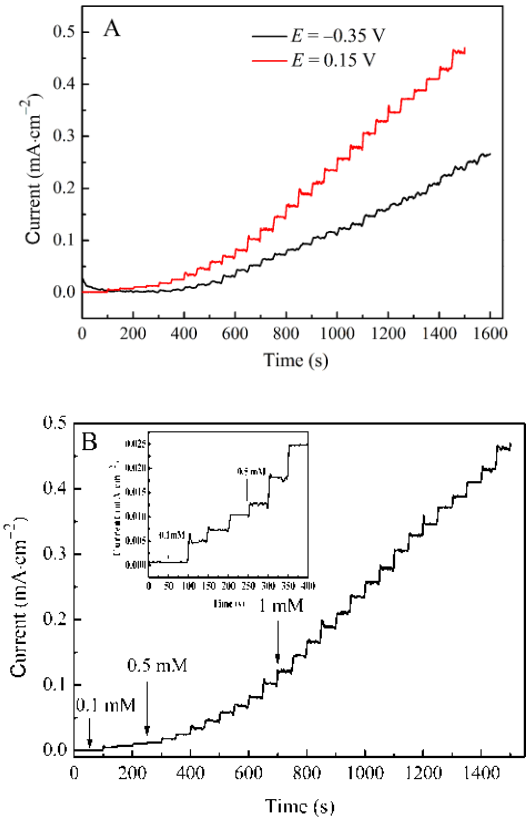

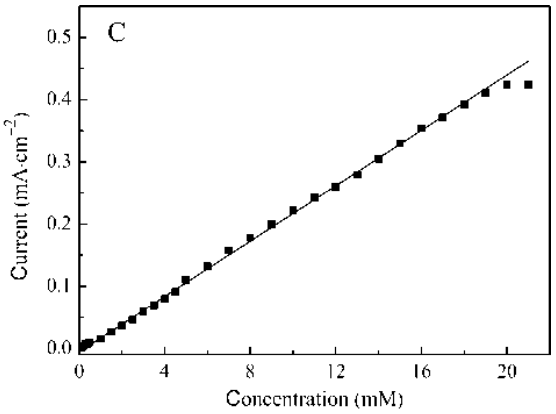

Figure 6. (A) Amperometric response of $Pt_{70}Cu_{30}$GCE electrode at –0.35 V and 0.15 V with successive additions of glucose to 0.1 M PBS containing 0.15 M NaCl (pH=7.4). (B) Amperometric response of $Pt_{70}Cu_{30}$GCE electrode examined in 0.1 M PBS containing 0.15 M NaCl (pH=7.4) with sequential additions of glucose at a constant potential at 0.15 V. Inset is the enlarged amperometric responses of the curve during 0-400 s. (C) The linear relationship between the response current with the glucose concentration.

Table 1. Comparison of different electrode materials for non-enzymatic glucose sensors

Electrode material	Linear range (mM)	Detection limit (μM)	Sensitivity ($\mu A \cdot mM^{-1} \cdot cm^{-2}$)	Reference
Nanoporous PtCu	0.6~15	50	10.6	[22]
Pt nanoflower	1~16	48	1.87	[2]
PtPb networks	up to16	Not application	10.8	[31]
Mesoporous Pt	0~10	Not application	9.6	[32]
PdCu nanoparticle	up to18	Not application	48	[12]
$Pt_{0.7}Co_{0.3}$/C	0.1~14.2	30	73.6	[7]
PtAu nanowires	0.02~0.14	Not application	101.2	[33]
PtPb nanowires array	up to11	8	11.3	[34]
$Pt_{70}Cu_{30}$ nanostrands	0.1~19	25	23	this work

With times going on, the increased amount of current density at –0.35 V tends to decline gradually with the incremental of glucose concentration. However, the current respond at 0.15 V aggrandizes linearly with the addition of glucose. This phenomenon can be interpreted as follows: at the low potential of –0.35 V, the glucose cannot be fully oxidized and thus intermediates form on the electrode surface, which hinders some of active surface sites and results in the decrease of the amperometric responses to the glucose concentration. But, when the electrode potential was at 0.15 V,

the glucose and its intermediates could be continuously oxidized on the surface of PtCu. On the basis of the higher current response and better linear relationship, 0.15 V was selected as the optimal detection potential.

Fig. 6B demonstrates the representative amperometric responses of the $Pt_{70}Cu_{30}$GCE electrode to glucose, which was performed by adding glucose step-wise into the stirred constantly solution containing 0.1 M PBS and 0.15 M NaCl at 0.15 V. After adding glucose into the stirred solution, a fast and remarkable response was presented for $Pt_{70}Cu_{30}$ GCE electrode, indicating that the response of the prepared electrode to glucose oxidation was sensitive and rapid. Fig. 6C shows a calibration curve of current response versus glucose concentrations. It has a linear glucose concentration in the range of 0.1 to 19 mM (R^2=0.99865) with the sensitivity of 23 $\mu A \cdot mM^{-1} \cdot cm^{-2}$ and the detection limit of 25 μM based on a signal to noise ratio of 3. The performance of our sensor is superior to those reported in other literatures listed in Table 1, which suggests that the $Pt_{70}Cu_{30}$ electrode is prospective for analytical application.

3.4. Stability, reproducibility and anti-interference ability of the electrode

The long-term stability is a significant factor for estimating the performance of a non-enzymatic glucose sensor.

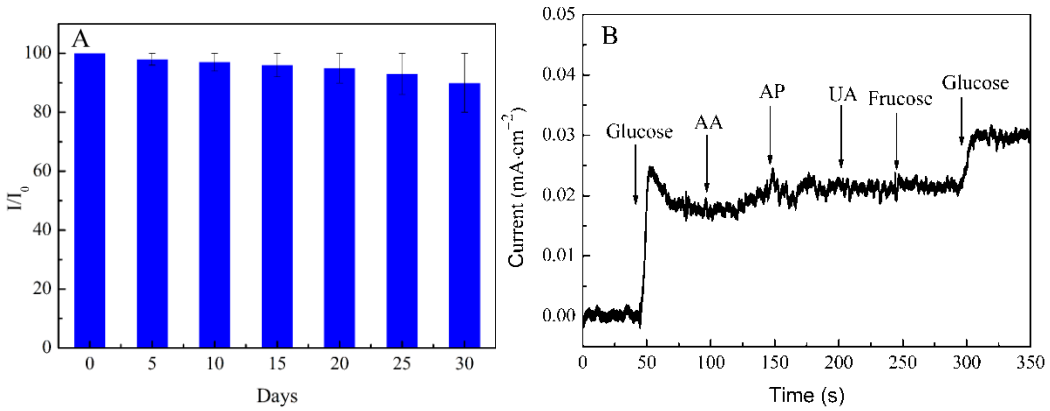

Figure 7. (A) Stability of $Pt_{70}Cu_{30}$ electrode kept in environmental conditions during a month for glucose detected; (B) Effect of interferences on amperometric response of the $Pt_{70}Cu_{30}$GCE electrode in a 0.1 M PBS containing 0.15 M NaCl (PH=7.4) with successive additions of 1 mM glucose, 1 mM AA, 1 mM AP, 1 mM UA, 1 mM fructose and 1 mM glucose; applied potential: 0.15 V.

The stability of the proposed sensor based on $Pt_{70}Cu_{30}$GCE electrode was examined by measuring its current response to 10 mM glucose every 5 days within a 30-day period. As shown in Fig. 7A, only 10% loss was observed in the current signal, which suggested a well long-term stability. The current responses for 10 mM glucose were measured 20 times using the same electrode with only a relative standard deviation (RSD) of 3.5%. The reproducibility of the $Pt_{70}Cu_{30}$GCE electrode was

evaluated by testing five identically prepared electrodes with a RSD of 2.8%, suggesting the reliability of this method.

It is known that the interfering electrochemical signals caused by the oxidation of endogenous substances such as ascorbic acid, acetamidophenol, uric acid and fructose may influence the detection of glucose. Thus, the ability of distinguishing target analyte from the interfering species is a very important parameter for an enzyme-less glucose sensors. Fig. 7B displays the amperometric response of the $Pt_{70}Cu_{30}$GCE electrode associated with the successive addition of 1 mM glucose, 1 mM AA, 1 mM AP, 1 mM UA, 1 mM fructose and 1 mM glucose in a stirred 0.1 M PBS solution containing 0.15 M NaCl at the potential of 0.15 V. From Fig. 7B, only inappreciable response signals of interfering species (fructose, AP, UA and AA) were observed when compared to glucose, which reveals the good anti-interference ability of the $Pt_{70}Cu_{30}$GCE electrode.

3.5. Real sample analysis

To evaluate the reliability in practical application, the $Pt_{70}Cu_{30}$GCE electrode was applied to detection of the concentration of glucose of diabetic and healthy people which were obtained from the local hospital. The recovery was measured by adding 1 mM glucose independently into the solution containing serum. The results are presented in Table 2.

Table 2. Amperometric determination of glucose in human blood serum samples by $Pt_{70}Cu_{30}$GCE electrode

Sample	Concentration (mM)	Reference values	RSD (n=3) (%)	Added (mM)	Found (mM)	Recovery (%)
1	5.2	5.28	2.8	1	6.1	98.4
2	5.9	5.95	1.2	1	6.8	98.6
3	6.8	6.91	2.9	1	7.9	101.3
4	7.7	7.75	0.9	1	8.5	97.7
5	11.8	11.93	2.6	1	12.7	99.2

It shows that the $Pt_{70}Cu_{30}$ electrode gives recoveries in the range of 97.7~101.3%, which demonstrates that the sensor based on $Pt_{70}Cu_{30}$ has the potential to be used for measuring glucose in real samples.

4. CONCLUSIONS

In summary, a sensitive non-enzymatic glucose sensor based on bimetallic Pt_xCu_{1-x} nanostrands electrode has been developed by a facile and effective wet chemical route. This class of modified electrode exhibits considerably enhanced electrocatalytic activity towards glucose oxidation compared to pure Pt nanostrands modified electrode prepared with the similar procedure. Because of its large

active area, good electrical conductivity and synergetic effects between the alloyed PtCu atoms, the $Pt_{70}Cu_{30}$GCE electrode presented a wide liner range from 0.1 to 19 mM and exhibited a good sensitivity of 23 $\mu A \cdot mM^{-1} \cdot cm^{-2}$ with a detection limit of 25 μM. In addition to the catalytic activities, the $Pt_{70}Cu_{30}$GCE electrode has the advantages of ease in preparation, inexpensive spend, outstanding reproducibility and perfect specificity to glucose with common interferences. These prominent properties of the proposed sensor make it a potential candidate for glucose detection in blood sample.

ACKNOWLEDGEMENTS
Tingting Guo and Yu Zhang contributed equally to this work. This work was financially supported by the National Natural Science Foundation of China (51271074) and (21305121).

References

1. http://www.who.int/mediacentre/factsheets/fs312/en/, 2011.
2. M.Q. Guo, H.S. Hong, X.N. Tang, H.D. Fang and X.H. Xu, *Electrochim. Acta*, 63 (2012) 1.
3. Z. Fan, B. Liu, X. Liu, Z. Li, H. Wang, S. Yang and J. Wang, *Electrochim. Acta*, 109 (2013) 602.
4. L.M. Lu, H.B. Li, F. Qu, X.B. Zhang, G.L. Shen and R.Q. Yu, *Biosens. Bioelectron.*, 26 (2011) 3500.
5. J. Luo, S. Jiang, H. Zhang, J. Jiang and X. Liu, *Anal. Chim. Acta*, 709 (2012) 47.
6. A. Heller and B. Feldman, *Accounts Chem. Res.*, 43 (2010) 963.
7. Q. Sheng, H. Mei, H. Wu, X. Zhang and S. Wang, *Sensor. Actuat. B: Chem.*, 207 (2015) 51.
8. Y. Li, X. Niu, J. Tang, M. Lan and H. Zhao, *Electrochim. Acta*, 130 (2014) 1.
9. X. Niu, M. Lan, C. Chen and H. Zhao, *Talanta*, 99 (2012) 1062.
10. F. Xiao, Y. Li, H. Gao, S. Ge and H. Duan, *Biosens. Bioelectron.*, 41 (2013) 417.
11. Y. Yu, Y. Yang, H. Gu, T. Zhou and G. Shi, *Biosens. Bioelectron.*, 41 (2013) 511.
12. M. Yuan, A. Liu, M. Zhao, W. Dong, T. Zhao, J. Wang and W. Tang, *Sensor. Actuat. B: Chem.*, 190 (2014) 707.
13. K.E. Toghill, L. Xiao, M.A. Phillips and R.G. Compton, *Sensor. Actuat. B: Chem.*, 147 (2010) 642.
14. C. Xu, Y. Liu, F. Su, A. Liu and H. Qiu, *Biosens. Bioelectron.*, 27 (2011) 160.
15. X. Cao, N. Wang, S. Jia and Y. Shao, *Anal. Chem.*, 85 (2013) 5040.
16. P.H.Hindle, S.Nigro, M.Asmussen and A.C.Chen, *Electrochem. Commun.*, 10 (2008) 1438.
17. L. Dai, S. Mo, Q. Qin, X. Zhao and N. Zheng, *Small*, 12 (2016) 1572.
18. N. Moghimi and K.T. Leung, *Anal. Chem.*, 85 (2013) 5974.
19. A.K. Wanekaya, W. Chen, N.V. Myung and A. Mulchandani, *Electroanal.*, 18 (2006) 533.
20. K.B. Male, S. Hrapovic, Y. Liu, D. Wang and J.H.T. Luong, *Anal.Chim. Acta*, 516 (2004) 35.
21. Y. Zhang, L. Su, D. Manuzzi, H.V.E. de los Monteros, W. Jia, D. Huo, C. Hou and Y. Lei, *Biosens. Bioelectron.*, 31 (2012) 426.
22. S. Chen, R. Yuan, Y. Chai and F. Hu, *Microchim. Acta*, 180 (2012) 15.
23. M. Jin, H. Zhang, J. Wang, X. Zhong, N. Lu, Z. Li, Z. Xie, M.J. Kim and Y. Xia, *ACS Nano.*, 3 (2012) 2566.
24. T. Schmidt, H. Gasteiger, G. Stäb, P. Urban, D. Kolb and R. Behm, *J. Electrochem. Soc.*, 145 (1998) 2354.
25. F. Xiao, F. Zhao, D. Mei, Z. Mo and B. Zeng, *Biosens. Bioelectron.*, 24 (2009) 3481.
26. A. Habrioux, E. Sibert, K. Servat, W. Vogel, K.B. Kokoh and N. Alonso-Vante, *J. Phys. Chem. B*, 111 (2007) 10329.
27. V.R. Stamenkovic, B. Fowler, B.S. Mun, G. Wang, P.N. Ross, C.A. Lucas and N.M. Markovic, *Science*, 315 (2007) 493.

28. Q. Sun, Z. Ren, R. Wang, N. Wang and X. Cao, *J. Mater. Chem.*, 21 (2011) 1925.
29. S. Park, S. Park, R.A. Jeong, H. Boo, J. Park, H.C. Kim and T.D. Chung, *Biosens. Bioelectron.*, 31 (2012) 284.
30. Y. Ding, Y. Wang, L. Zhang, H. Zhang andY. Lei, *J. Mater. Chem.*, 22 (2012) 980.
31. J.P. Wang, Dan F. Thomas and A. Chen, *Anal. Chem.*, 80 (2008) 997.
32. S. Park, T.D. Chung and H.C. Kim, *Anal. Chem.*, 75 (2003) 3046.
33. C.C. Chem. CommunMayorga-Martinez, M. Guix, R.E. Madrid and A. Merkoçi, *Chem. Commun.*, 48 (2012) 1686.
34. Y. Bai, Y. Sun and C. Sun, *Biosens. Bioelectron.*, 24 (2008) 579.